

## GLOBAL SIGNIFICANCE OF $\delta^{34}\text{S}$ OF INORGANIC AND ORGANIC SULFUR PHASES ACROSS THE PERMIAN-TRIASSIC TRANSITION

H. Grotheer<sup>1,#</sup>, P. F. Greenwood<sup>1,2</sup>, M. T. McCulloch<sup>2</sup>, M. E. Böttcher<sup>3</sup>, R. E. Summons<sup>4</sup>, K. Grice<sup>1</sup>

<sup>1</sup>Curtin University, Australia; <sup>2</sup>University of Western Australia, Australia; <sup>3</sup>Leibniz Institute for Baltic Sea Research, Germany; <sup>4</sup>Massachusetts Institute of Technology, USA; #corresponding author: h.grotheer@curtin.edu.au

The ~251 Ma ago Permian/Triassic (P-Tr) extinction was the most severe of the Phanerozoic extinctions, with a disappearance of 95 % of marine species (e.g. Erwin et al., 2002) over a relatively short time interval ( $\sim 60 \pm 48$  kyr; Burgess et al., 2014). Still, no consensus about the causes exists, with the most popular explanations including i) massive volcanic activity associated with the Siberian flood basalts; and ii) global anoxia and euxinia (e.g. Grice et al., 2005; Whiteside and Grice, 2016) during the formation of the supercontinent Pangea. Either of these processes could have been responsible for the profound impact on the global S-cycle shown by isotopic variations of inorganically bound S-phases (sulfate and pyrite; e.g. Kaiho et al., 2006; Gorjan et al., 2007). Here we complement the isotopic analysis of inorganic S with bulk organic S and, for the first time, organosulfur compounds in two Permian-Triassic boundary (PTB) sections from I) a carbonate dominated Global Stratotype Section and Point (GSSP) at Meishan-1 (South China) and II) a mud-rock sequence at Hovea-3 (Western Australia).

The Meishan-1 PTB section shows an isotopically distinct event horizon beginning at the top of bed 22 (~ 4 m below P-Tr extinction) and leading up to the top of bed 24 (just below the extinction and ~40 cm below PTB). In the event horizon total reduced inorganic sulfur (TRIS  $\approx$  pyrite) shows a profound  $^{34}\text{S}$  enrichment (from -30 to -13 ‰). Compound specific  $\delta^{34}\text{S}$  analysis of dibenzothiophene (DBT) reveals a simultaneous  $^{34}\text{S}$  depletion (from -17 to -24 ‰). Following the extinction (located in bed 25)  $\delta^{34}\text{S}$  of TRIS and DBT return to near pre-event levels whereas kerogen S becomes depleted by 12 ‰. This novel data set suggests that DBT represents a sub-fraction of kerogen S that was isotopically sensitive to the changes in depositional setting (e.g. water column redox conditions etc.) during the extinction event, unlike the bulk kerogen which showed constant  $\delta^{34}\text{S}$  values. An inverse relationship evident in the  $\delta^{34}\text{S}$  profiles of TRIS and DBT suggests the disproportionation of a common reduced S source ( $\text{HS}_x^-$ ). This isotopic excursion coincided with an increase in abundance of organic sulfur, reflected by decreasing TRIS/(TRIS+KerogenS) values, which likely favoured OM sulfurisation over pyritisation.

A more moderate  $\sim 4$  ‰  $^{34}\text{S}$  depletion of TRIS and  $\sim 1.5$  ‰  $^{34}\text{S}$  enrichment of DBT was measured across the relatively condensed PTB section suspected in Hovea-3. The direction and lower magnitude of the  $\delta^{34}\text{S}$  variations was in contrast to the Meishan data, and may be due to higher abundances of kerogen S and more so inorganic S deposited at this site. The contrasting  $\delta^{34}\text{S}$  behaviour of the different S-phases across these 2 PTB sections implies a greater sensitivity to local basin conditions (e.g. water column redox conditions) or lithology than coincident global events such as volcanic activity (e.g. elevated influx of volcanic S species).

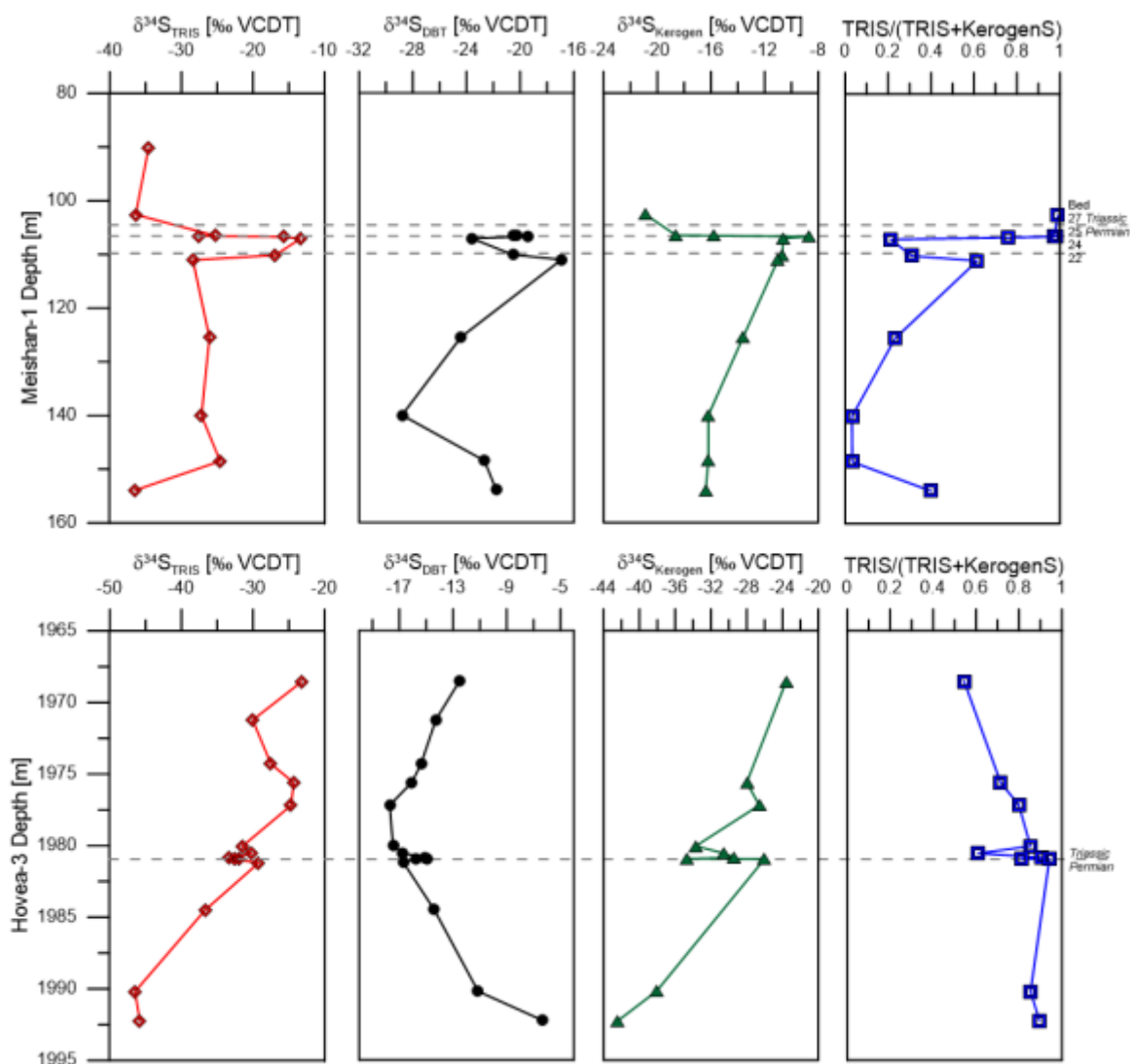


**Figure 1**  $\delta^{34}\text{S}$  profile of total reduced sulfur (TRIS, red), dibenzothiophene (DBT, black), and kerogen bound S (green) as well as fractional abundance of inorganic vs organic S (TRIS/(TRIS+KerogenS), blue) for PTB sections in Meishan-1 (top, extinction in bed 25, PTB in bed 27, implied as dashed lines) and Hovea-3 (bottom, PTB indicated as dashed line).

## References

- Burgess, S.D., Bowring, S.A., Shen, S.Z., 2014. High-precision timeline for Earth's most severe extinction. *Proceedings of the National Academy of Sciences* 111, 3316–3321.
- Erwin, D.H., Bowring, S.A., Yugan, J., 2002. End-Permian mass extinctions: A review. *Geological Society of America Special Paper* 365, 363–383.
- Gorjan, P., Kaiho, K., Kakegawa, T., Niitsuma, S., Chen, Z.Q., Kajiwara, Y., Nicora, A., 2007. Paleoredox, biotic and sulfur-isotopic changes associated with the end-Permian mass extinction in the western Tethys. *Chemical Geology* 244, 483–492.
- Grice, K., Cao, C., Love, G.D., Böttcher, M.E., Twitchett, R.J., Grosjean, E., Summons, R.E., Turgeon, S.C., Dunning, W., Jin, Y., 2005. Photic zone euxinia during the Permian-triassic superanoxic event. *Science* 307, 706–709.
- Kaiho, K., Kajiwara, Y., Chen, Z.-Q., Gorjan, P., 2006. A sulfur isotope event at the end of the Permian. *Chemical Geology* 235, 33–47.
- Whiteside, J.H., Grice, K., 2016. Biomarker Records Associated with Mass Extinction Events. *Annual Review of Earth and Planetary Sciences* 44, 581–612.